50% of this area in March) is reduced. However, the increases in stratospheric halogen loading due to anthropogenic emissions has contributed significantly to the springtime decrease since the 1970s. The observed decadal decrease in column O_3 values in March north of 63° N may contain a large (>50%) contribution from slow, year-round, halogen-catalysed depletion.

These results have implications for future levels of ozone in the Arctic region. Although the amount of PSC-induced chemical depletion within the vortex may be enhanced due to stratospheric cooling[24], the main factor determining the average ozone column to date in a given winter is dynamics. This transport is affected by interannual variability, but may also be subject to a trend—for example, due to stratospheric O_3 decrease or other climate-related effects. Possible future circulation changes (for example, those that make the Arctic vortex more Antarctic-like) could significantly change mean wintertime ozone levels by transport alone. Also, while Shindell *et al.*[24] pointed out the potential feedback between stratospheric cooling which may delay the recovery of Arctic ozone as halogen levels decrease, the contribution of halogens to the decadal decrease in ozone in the larger extra-vortex region may be expected to follow the halogen loading more closely, unless cooling extends PSC activation outside the vortex. □

Received 26 October 1998; accepted 11 June 1999.

1. Newman, P. A. *et al.* Anomalously low ozone over the Arctic. *Geophys. Res. Lett.* **24,** 2689–2692 (1997).
2. Fioletov, V. E. *et al.* Long-term ozone decline over the Canadian Arctic to early 1997 from ground-based and balloon observations. *Geophys. Res. Lett.* **24,** 2705–2708 (1997).
3. Rex, M. *et al.* Prolonged stratospheric ozone loss in the 1995–96 Arctic winter. *Nature* **389,** 835–838 (1997).
4. Müller, R. *et al.* Chlorine activation and ozone depletion in the Arctic vortex: Observations by the Halogen Occultation Experiment on the Upper Atmosphere Research Satellite. *J. Geophys. Res.* **101,** 12531–12554 (1996).
5. Müller, R. *et al.* Severe chemical ozone loss in the Arctic during the winter 1995–96. *Nature* **389,** 709–712 (1997).
6. Müller, R. *et al.* HALOE observations of the vertical structure of chemical ozone depletion in the Arctic vortex during winter and early spring 1996–1997. *Geophys. Res. Lett.* **24,** 2717–2720 (1997).
7. Manney, G. L. *et al.* Arctic ozone depletion observed by UARS MLS during the 1994–95 winter. *Geophys. Res. Lett.* **23,** 85–88 (1996).
8. Manney, G. L., Santee, M. L., Froidevaux, L., Waters, J. W. & Zurek, R. W. Polar vortex conditions during the 1995–96 Arctic winter: Meteorology and MLS ozone. *Geophys. Res. Lett.* **23,** 3203–3206 (1996).
9. Manney, G. L., Froidevaux, L., Santee, M. L., Zurek, R. W. & Waters, J. W. MLS observations of Arctic ozone loss in 1996–97. *Geophys. Res. Lett.* **24,** 2697–2700 (1997).
10. Sinnhuber, B. M., Langer, S., Klein, U., Raffalski, U. & Kunzi, K. Ground based millimeter-wave observations of Arctic ozone depletion during winter and spring of 1996/97. *Geophys. Res. Lett.* **25,** 3327–3330 (1997).
11. Hansen, G., Svenøe, T., Chipperfield, M. P., Dahlback, A. & Hoppe, U. P. Evidence of substantial ozone depletion in winter 1995/96 over northern Norway. *Geophys. Res. Lett.* **24,** 799–802 (1997).
12. Zurek, R. W., Manney, G. L., Miller, A. J., Gelman, M. E. & Nagatani, R. M. Interannual variability of the north polar vortex in the lower stratosphere during the UARS mission. *Geophys. Res. Lett.* **23,** 289–292 (1996).
13. Dobson, G. M. B. Observations of the amount of ozone in the earth's atmosphere and its relation to other geophysical conditions. *Proc. R. Soc. Lond. A* **129,** 411–433 (1930).
14. Hood, L. L., McCormack, J. P. & Labitzke, K. An investigation of dynamical contributions to midlatitude ozone trends in winter. *J. Geophys. Res.* **102,** 13079–13093 (1997).
15. Steinbrecht, W., Claude, H., Kohler, U. & Hoinka, K. P. Correlations between tropopause height and total ozone: Implications for long-term changes. *J. Geophys. Res.* **103,** 19183–19192 (1998).
16. Rood, R. B., Allen, D. J., Baker, W. E., Lamich, D. J. & Kaye, J. A. The use of assimilated stratospheric data in constituent transport calculations. *J. Atmos. Sci.* **46,** 687–701 (1989).
17. Lefèvre, F., Brasseur, G. P., Folkins, I., Smith, A. K. & Simon, P. Chemistry of the 1991–1992 stratospheric winter: Three-dimensional model simulations. *J. Geophys. Res.* **99,** 8183–8195 (1994).
18. Chipperfield, M. P. *et al.* Analysis of UARS data in the southern polar vortex in September 1992 using a chemical transport model. *J. Geophys. Res.* **101,** 18861–18881 (1996).
19. Chipperfield, M. P. Multiannual simulations with a 3D chemical transport model. *J. Geophys. Res.* **104,** 1781–1805 (1999).
20. Swinbank, R. & O'Neill, A. A stratosphere-troposphere data assimilation system. *Mon. Weath. Rev.* **122,** 686–702 (1994).
21. Lefèvre, F., Figarol, F., Carslaw, K. S. & Peter, T. The 1997 Arctic ozone depletion quantified from three-dimensional model simulations. *Geophys. Res. Lett.* **25,** 2425–2428 (1998).
22. Becker, G., Müller, R., McKenna, D. S., Rex, M. & Carslaw, K. S. Ozone loss rates in the Arctic stratosphere in the winter 1991/1992: Model calculations compared with Match results. *Geophys. Res. Lett.* **25,** 4325–4329 (1998).
23. World Meteorological Organization *Scientific Assessment of Ozone Depletion: 1994* (Rep. No. 7, Global Ozone Research and Monitoring Project, Geneva, 1995).
24. Shindell, D. T., Rind, D. & Lonergan, P. Increased polar stratospheric ozone losses and delayed eventual recovery owing to increasing greenhouse-gas concentrations. *Nature* **392,** 589–592 (1998).

Acknowledgements. We thank P. Newman for information about the 1998 TOMS data, H. Teyssèdre for TOMS calculations, and J. A. Pyle for help and support. This work was supported by the UK Natural Environment Research Council.

Correspondence and requests for materials should be addressed to M.P.C. (e-mail: martyn@lec.leeds.ac.uk).

2-Methylhopanoids as biomarkers for cyanobacterial oxygenic photosynthesis

Roger E. Summons*, Linda L. Jahnke, Janet M. Hope* & Graham A. Logan*

* *Australian Geological Survey Organisation, GPO Box 378, Canberra, ACT 2601, Australia*

† *Exobiology Biology Branch, NASA Ames Research Center, Moffett Field, California 94035, USA*

Oxygenic photosynthesis is widely accepted as the most important bioenergetic process happening in Earth's surface environment[1]. It is thought to have evolved within the cyanobacterial lineage, but it has been difficult to determine when it began. Evidence based on the occurrence and appearance of stromatolites[2] and microfossils[3] indicates that phototrophy occurred as long ago as 3,465 Myr although no definite physiological inferences can be made from these objects. Carbon isotopes and other geological phenomena[4,5] provide clues but are also equivocal. Biomarkers are potentially useful because the three domains of extant life—Bacteria, Archaea and Eukarya—have signature membrane lipids with recalcitrant carbon skeletons. These lipids turn into hydrocarbons in sediments and can be found wherever the record is sufficiently well preserved. Here we show that 2-methylbacteriohopanepolyols occur in a high proportion of cultured cyanobacteria and cyanobacterial mats. Their 2-methylhopane hydrocarbon derivatives are abundant in organic-rich sediments as old as 2,500 Myr. These biomarkers may help constrain the age of the oldest cyanobacteria and the advent of oxygenic photosynthesis. They could also be used to quantify the ecological importance of cyanobacteria through geological time.

In the Bacteria, bacteriohopanepolyols (BHP) are amphiphilic membrane biochemicals[6] that serve a regulating and rigidifying function similar to that of sterols in the Eukarya. The hydrocarbon skeletons of BHP are extremely refractory and resist biodegradation to become incorporated into kerogen or bound into sulphur-linked macromolecules. They also survive high geothermal gradients accompanying hydrocarbon generation and ultimately appear in petroleum as defunctionalized and stereochemically modified[7] 'geohopanes'. Although many aspects of the preservation of BHP are well understood, there remains uncertainty about the sources of BHP and environmental controls on their abundance and distribution. This study assesses the role of cyanobacteria as a source of fossil hopanoids.

Table 1 summarizes the hopanoid contents of cultured cyanobacteria and mat communities that we analysed, along with data extracted from the literature. The high polarity and complexity of the hydrophilic side chains of BHP[8] precludes a generalized gas chromatography–mass spectrometry (GC–MS) analysis that detects all hopanoids. Accordingly, we applied the methodology of ref. 9 (Fig. 1) in our survey of the occurrence of hopane skeletons in cultures and environmental samples. Structural variation in the hydrophobic pentacyclic triterpane skeleton of BHP appears to be very limited. Unsaturation (Δ6 and/or Δ11) is rare, but supplementary methyl substituents at the 2α, 2β and 3β positions of ring-A have been reported often and may indicate metabolism in some bacteria. Methylation at C3 has been reported for a variety of methanotrophic, methylotrophic and acetic bacteria[9,10]. Methylation at C2 is common in cyanobacteria[9,11], as shown in Table 1, although it is not exclusive to this group. Of those other bacteria that have been studied, 2-methylhopanoids have also been found in pink pigmented faculative methylotrophs (PPFMs) related to *Methylobacterium organophilum*[12] and some nitrogen-fixing bacteria

Table 1 Abundances (μg per g dry wt) of hopanols analysed in cultured cyanobacteria, a prochlorophyte and various environmental samples

Cyanobacterial cultures and environmental samples analysed in this study	C31 5	2-MeC31 6	C32 7	2-MeC32 8
Phormidium luridum UTEX 426 (CCAP 1462/2)			540	74
Chlorogloeopsis fritschii ATCC 27193			65	7
Synechococcus lividus ATCC 27180			155	95
Synechococcus ATCC 29534 (*Aphanothece halophitica*)			20	30
Synechococcus ATCC 27144 (*Anacystis nidulans*)	39	63	25	23
Gloeobacter violaceus ATCC 29082			450	650
Anabaena cylindrica ATCC 27899			68	
Fischerella sp. ATCC 29538			2	
Phormidium sp. 'OSS4' Octopus Spring, YNP	179	258	<1	23
Phormidium sp. 'RCG' Rabbit Creek, YNP			161	
Phormidium sp. 'RCO' Rabbit Creek, YNP			<1	
Phormidium sp. 'OSS3' Octopus Spring, YNP			45	
Chlorogloeopsis sp. 'LA' Norris Geyser Basin, YNP	286		374	
Calothrix sp. 'TSB' Twin Springs, YNP			255	
Oscillatoria limnetica (Y. Cohen), Solar Lake, Israel			40	
Oscillatoria sp. 'GN' (E. Munoz), Guerrero Negro, Mexico			<1	
Phormidium sp. 'GN' (E. Munoz), Guerrero Negro, Mexico			<1	
Oscillatoria sp. (L. Stal) Mellum Island, Germany			27	
Oscillatoria sp. 10mfx (J. Bauld) Shark Bay, Australia			18	
Octopus Spring *Synechococcus-Chloroflexus* 60 °C mat*	14	20	23	
Octopus Spring *Synechococcus-Chloroflexus* 55 °C mat*[16]	1	1	8	
Octopus Spring *Phormidium-Chloroflexus* 45 °C mat*	61	64	90	29
Fountain Paint Pot *Phormidium-Chloroflexus* 45 °C mat*	9	30	24	13
Rabbit Creek *Phormidium-Chloroflexus* 40 °C mat*	2	32	24	7
Shark Bay 'Smooth' Mat (J88/1 predom. *Microcoleus sp.*)†			1.2	
Shark Bay 'Tufted' Mat (J88/9 predom. *Lyngbya sp.*)†			0.7	
Shark Bay 'Smooth' Mat (J88/10 predom. *Microcoleus sp.*)†			0.7	
Shark Bay 'Tufted' Mat (J88/14 predom. *Lyngbya sp.*)†			20	
Shark Bay 'Pustular' Mat (J88/17 predom. *Entophysalis sp.*)†			1.0	
Data extracted from literature reports				
Prochlorothrix hollandica whole cells[11]			60	90
Prochlorothrix hollandica cell wall[11]			400	600
Prochlorothrix hollandica thylakoids[11]			940	1410
Nostoc sp. ATCC 27985‡[8]			250	‖
Nostoc muscorum B-1453-12b¶[26]			3x	7x
Nostoc sp. PCC 6720[27]	55	220	66	160
Scytonema sp. ATCC 29171‡[8]			100	‖
Synechococcus sp. PCC 6907[28]			135	72
Calothrix anomala[15]	15		<1	400
Schizothrix sp.[15]	2		130	<1
Anacystis montana[15]	<1		44	180
Oscillatoria rubescens[15]	<1		430	<1
Gloeobacter sp.[15]	<1		<1	2700
Various species (9)‡			3–140	
Various species (3)‡[8]	<1		<1	

* Indicates relative amounts of bacteriohopanol in mats and are for top photic zone (~1 mm for *Synechococcus* and up to 1 cm for *Phormidium*) and do not account for high levels of silica associated with dry weight.
† Indicates data do not account for high levels of $CaCO_3$ associated with dry weight.
‖ Indicates an x-methylhopanol was detected but the identity and proportion are unspecified.
¶ Indicates only compound ratios and not absolute abundances available.
# Indicates that a 2-methyl-C_{30} hopanol precursor was also reported.
‡ Indicates that the original 1984 methodology was used and this may have underestimated BHP contents (M. Rohmer, personal communication).

of the genera *Azotobacter* and *Beijerinkia*[13]. However, the predominant 2-methylhopanoids in these organisms are diplopterols and diploptenes, which are C_{31} alcohols and hydrocarbons. Only trace amounts of 2-methyl-BHP have been identified in *M. organophilum*[14]. This has significant implications for their preservation potential, because diplopterols readily dehydrate to diploptenes, which have very limited capacity to be incorporated into kerogen. BHP and 2-methyl-BHP, on the other hand, have multiple functional groups through which they can be incorporated into the kerogen matrix and preferentially preserved. Although 2-methyl-BHP may be found in unstudied taxa in the future, the cyanobacterial lineage currently comprises the only known quantitatively significant source[9,11,15,16] with a conduit to selective preservation.

The C_{32} hopanol (alcohol precursor of type 7 in Fig. 1) is by far the most common BHP derivative encountered in cyanobacteria. Its BHP precursors are probably the source of the C_{32} carboxylic acid and C_{31} hydrocarbon that are the most widespread geohopanoids in recent sediments. Around 43% of the listed samples contain 2-methyl analogues (6 and 8). Four out of five mats from the Yellowstone National Park hydrothermal environment contained significant 2-methyl-BHP, although none of five samples from the hypersaline environments of Shark Bay did. Although the present sample set gives limited coverage of modern environments, species that have been cultured include one prochlorophyte and span a taxonomically diverse spectrum of cyanobacteria. The Yellowstone *Phormidium* conophyton mats that we studied all had abundant 2-methyl-BHP. These are the possible modern analogues for the conophyton stromatolites that have a sedimentary record reaching back 2,700 Myr (ref. 2). However, note that biomarker probes for the antiquity of cyanobacteria are unidirectional, as 2-methyl-BHP are not found in all cultured species nor all mats.

The sedimentary conversion of BHP to the C_{27}-C_{35} geohopane series (3 in Fig. 1) has been extensively studied in connection with the application of these biomarkers to petroleum exploration[7]. The burial fate of 2-methyl-BHP is virtually identical to that of BHP except that the 2β-methyl configuration of the original biochemicals (2 in Fig. 1) is progressively converted to the more thermodynamically stable 2α-methyl configuration (4 in Fig. 1) in the 2-methyl geohopane series[17]. Despite this, we need to be cautious in how we validate fossil hydrocarbons. Establishing that they are indigenous to the host rock requires close attention to a variety of factors, as these compounds are mobile. Low levels of metamorphism, high contents of associated kerogen, covariance of the $\delta^{13}C$ of kerogen and bitumen, remoteness from younger oil-prone rocks and distinctive compound assemblages indicate syngeneity, especially when there is convergence of multiple lines of evidence for a particular sample. To the best of our knowledge, all

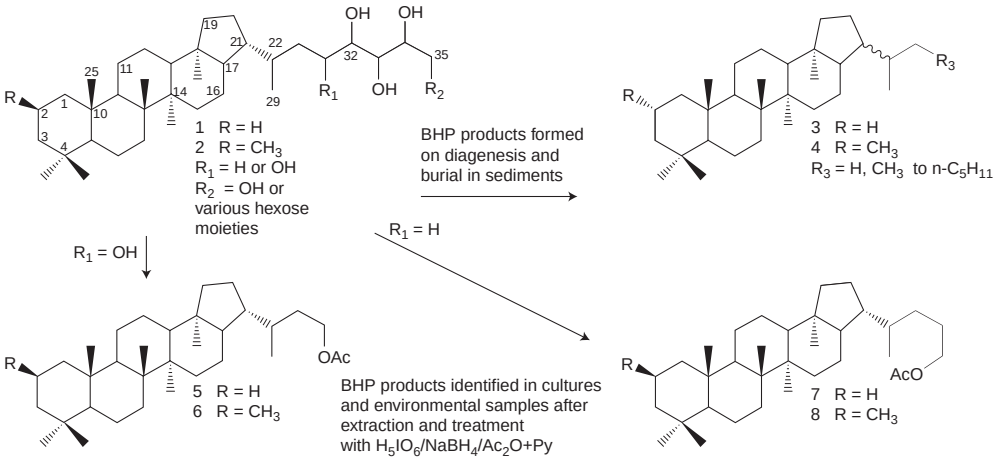

Figure 1 Structures of bacteriohopanepolyols (1, 2) typical of those found in cyanobacteria and their geohopane analogues recognized in sediments and petroleum (3, 4). BHP from cultures and environmental samples were chemically reduced to hopanol acetates of types 5–8 and analysed by GC–MS.

the bitumens listed in Table 2 are indigenous to their host formations, whereas all the oils are derived from specific source rocks of the designated ages.

The data shown in Table 2 confirm earlier observations[17,18] that higher relative abundances of 2-methylhopanes, expressed here as a 2-methylhopane index, are a distinctive feature of oils and bitumens derived from carbonate rocks. Moreover, there are high relative abundances of 2-methylhopanes in Proterozoic (>550 Myr) sediments of all lithologies compared to their Phanerozoic (<550 Myr) counterparts. Our data indicate that burial temperature strongly affects the 2-methylhopane index, because all immature samples analysed had low values. This indicates that generation requires cracking from chemically-bound precursors and independently supports their origin from BHP rather than diplopterols or diploptenes. The data for mature samples confirm previous observations that oils from carbonate source rocks have the highest 2α-methylhopane indices[17]. Such sediments frequently form in warm, low-latitude, shallow-water continental shelves, coastal lagoons, and other restricted marine settings. They also form in playa and saline lakes, as exemplified by the samples from the Early Cambrian Observatory Hill Formation, which had the highest 2-methylhopane indices we have encountered so far. Modern settings of this type are noted for the development of taxonomically diverse cyanobacterial mats[19,20] and moderate-to-high rates of organic matter accumulation[20]. It is likely that this has been the case for at least the past 2,500 Myr. Given the occurrence of 2-methyl-BHP in a wide variety of cyanobacterial taxa and cyanobacterial mats, a high abundance of 2-methylhopanes is expected in carbonate-derived oils of any age. Organic-rich shales, on the other hand, form in more open and distal marine settings including shelves, slopes and deltas, prone to clastic sediment inputs. In modern and Phanerozoic settings such as these, algae are the prime autotrophs with sedimentary carbon supplemented with inputs from allochthonous terrestrial organic matter. Planktonic and picoplanktonic cyanobacteria may be responsible for significant primary productivity in the modern ocean and our data indicate that they would have been more significant in times past, particularly in the Proterozoic[21]. Oils and bitumens from Proterozoic shales have higher 2-methylhopane indices (5–18.7%) than the mature Phanerozoic shale samples that we analysed (0.3–9%).

Given that 2-methyl-BHP are prominent lipids in cyanobacteria and cyanobacteria-dominated environmental samples, it is evident that 2-methyl-BHP and their derivative 2α-methylhopanes also comprise a molecular record for oxygenic photosynthesis, as this is their preferred physiology. The high abundance of derivative 2α-methylhopanes in bitumens from the 2,500 Myr Mt McRae Shale of the Hamersley basin provides direct evidence for oxygenic photosynthesis at this time and supports microfossil and other geological evidence that the process predates this. The Hamersley basin samples are also significant for another reason. Their sediment extracts extend the molecular biomarker record to the base of the Palaeoproterozoic, and are 700 Myr older than the oldest known biomarkers[22]. The Mt McRae Shale meets most of the important syngeneity criteria, especially with respect to having high organic carbon contents (0.5–6.9%) and hydrocarbon stereoisomer patterns that correlate well with other estimates of their thermal history (Ro ≈ 1.5–1.9). The Pilbara craton of Western Australia, location of the Hamersley basin, is also remote from any known Phanerozoic petroleum sources. Although it is difficult to find suitably preserved Archaean (>2,500 Myr) samples, recent work on fluorescing, fluid-bearing inclusions in quartz crystals in sandstones of this age, and older, indicate that some hydrocarbons generatesd at this time may have been preserved[23] and are likely to

Table 2 2-Methylhopane indices for well characterized oils and sedimentary bitumens

Formation	Lithology	Age (Myr)	Index
Mt. McRae Shale (3)	Shale	~2,500	12.5
Wollogorang Fm. (2)	Shale	~1,730	12.0
Barney Creek Fm. (6)	Shale	~1,640	8.5
Balbirini Fm.	Shale	~1,600	9.0
Yalco Fm. (1)	Shale	~1,485	14.7
McMinn Fm. (1)	Shale	~1,400	5.8
Nonesuch Fm. (2)	Shale	~1,000	4.7
Kwagunt Fm. (2)	Marl	~850	10.9
Kwagunt Fm. (1)	Shale	~850	18.7
Bitter Springs Fm (3)	Marl	~830	6.6
Draken Fm. (2)	Carbonate	~720	8.8
Ungoolya Fm. (4)	Shale	~560	6.7
Pertatataka Fm. (3)	Shale	~560	4.9
Shuram Fm. (1)	Marl	~560	12.7
Athel Fm. (1)	Marl	~550	11.2
Huqf Group oil (2)	Carbonate	~550	10.9
Observatory Hills Fm. (4)	Carb./evap.	530–540	32.4
Ouldburra Fm. (4)	Carbonate	530–540	9.9
Inca Fm.* (1)	Shale	505–510	2.4
Horn Valley Fm. (1)	Shale	460–485	5.3
Milligans Fm. (2)	Shale	330–345	9.4
Phosphoria Fm. oil (1)	Shale	270–300	0.5
Cooper basin oils (4)	Coal	250–270	4.0
Bowen basin oils (12)	Coal	250–270	8.9
Vulcan sub-basin oil (2)	Shale	150–160	4.5
Barrow sub-basin oil (2)	Shale	150–160	4.5
North Sea oil (1)	Shale	150–160	2.5
Julia Ck. Fm.* (1)	Shale	97–108	0.6
Taranaki basin (1)	Shale	61–65	0.3
Monterey Fm.* (2)	Carbonate	17–24	5.0
Monterey Fm.* (1)	Shale	6–8	0.9

* Samples above the oil window (see Methods).

hold a valid chemical fossil record[24].

Cyanobacterial BHP and 2-methyl-BHP may have oceanographic and palaeo-oceanographic applications as well, particularly with respect to evaluation of cyanobacterial primary productivity and their importance for the marine nitrogen and carbon cycles[25]. As biomarkers such as BHP and chlorophylls carry ^{13}C and ^{15}N signatures[16], their usefulness as tracers in modern aquatic and marine environments is significantly broadened. □

Methods

Total lipid extracts from cultures and environmental samples were analysed using a procedure modified and improved after ref. 8. Periodic acid oxidation followed by $NaBH_4$ reduction converted BHP to simpler hopanols amenable to purification by thin-layer chromatography and GC–MS analysis as acetate derivatives. BHP lacking a gem-diol function evade detection. The total number of culture samples with suitable data was 42 and, of these, only 6 failed to yield detectable hopanol. The data in Table 1 are from this study or directly extracted or calculated from published quantitative data.

The data for fossil hopanoids shown in Table 2 was derived from GC–MS–MS analyses[5] and based on the *m/z* 412 → 191 transition for αβ-hopane (3 in Fig. 1, R_3 = H) and *m/z* 426 → 205 for its 2α-methyl analogue (4, R_3 = H). These are expressed as the 2-methylhopane index = % 4/4+3. Accompanying C_{28}–C_{36} homohopanes (R = CH_3, R_3 = CH_3 to C_5H_7) were examined using the *m/z* 205 ion chromatograms and confirmed the relationships expressed here for the C_{30} and 2α-methyl C_{31} species. Age and lithology assignments for Phanerozoic samples were derived from AGSO databases. Assignments for Proterozoic sediments are primarily based on ref. 5, updated where possible. Numbers in parentheses indicate (*n*) samples of each rock unit. All samples are mature for oil generation except those marked with asterisks, which are above the oil window. Low 2α-methylhopane indices in these samples indicates incomplete release by thermal cracking of C_{35} and 2-Me C_{36} moieties bound in kerogen.

Received 23 March; accepted 11 June 1999.

1. Blankenship, R. E. & Hartman, H. The origin and evolution of oxygenic photosynthesis. *Trends Biochem. Sci.* **23,** 94–97 (1998).
2. Walter, M. R. in *Early Life on Earth* (ed. Bengtson, S.) 270–286 (Columbia Univ. Press, New York, 1994).
3. Schopf, J. W. Microfossils of the early Archean Apex Chert: New evidence of the antiquity of life. *Science* **260,** 640–646 (1993).
4. Buick, R. The antiquity of oxygenic photosynthesis: Evidence from stromatolites in sulfate-deficient Archaean lakes. *Science* **255,** 74–77 (1992).
5. Schopf, J. W. & Klein, C. *The Proterozoic Biosphere. A Multidisciplinary Study* (Cambridge Univ. Press, 1992).
6. Jürgens, U. J., Simonin, P. & Rohmer, M. Localisation and distribution of hopanoids in membrane systems of the cyanobacterium *Synechocystis* PCC 6714. *FEMS Microbiol. Lett.* **92,** 285–288 (1992).
7. Peters, K. E. & Moldowan, J. M. *The Biomarker Guide—Interpreting Molecular Fossils in Sediments and Petroleum* (Prentice-Hall, Englewood Cliffs, New Jersey, 1992).
8. Rohmer, M. The biosynthesis of triterpenoids of the hopane series in the eubacteria: a mine of new enzyme reactions. *Pure Appl. Chem.* **65,** 1293–1298 (1993).
9. Rohmer, M., Bouvier-Navé, P. & Ourisson, G. Distribution of hopanoid triterpenes in prokaryotes. *J. Gen. Microbiol.* **130,** 1137–1150 (1984).
10. Zundel, M. & Rohmer, M. Prokaryotic triterpenoids 3. The biosynthesis of 2β-methylhopanoids and 3β-methylhopanoids of *Methylobacterium organophilum* and *Acetobacter pasteurianus* spp. *pasteurianus*. *Eur. J. Biochem.* **150,** 35–39 (1985).
11. Simonin, P., Jürgens, U. J. & Rohmer, M. Bacterial triterpenoids of the hopane series from the prochlorophyte *Prochlorothrix hollandica* and their intracellular localisation. *Eur. J. Biochem.* **241,** 865–871 (1996).
12. Knani, M., Corpe, W. A. & Rohmer, M. Bacterial hopanoids from pink-pigmented facultative methylotrophs and from green plant surfaces. *Microbiology* **140,** 2755–2759 (1994).
13. Vilchèze, C., Llopiz, P., Neunlist, S., Poralla, K. & Rohmer, M. Prokaryotic triterpenoids: new hopanoids from the nitrogen-fixing bacteria *Azotobacter vinelandii*, *Beijerinckia indica* and *Beijerinckia mobilis*. *Microbiology* **140,** 2794–2753 (1994).
14. Renoux, J.-M. & Rohmer, M. Prokaryotic triterpenoids. New bacteriohopane tetrol cyclitol ethers from methylotrophic bacterium *Methylobacterium organophilum*. *Eur. J. Biochem.* **151,** 405–410 (1985).
15. Hermann, D. Des biohopanoïdes aux géohopanoïdes. Une approche de la formation des fossiles moléculaires de triterpénoïds en série hopane. Thesis, Univ. Haute-Alsace (1995).
16. Summons, R. E., Jahnke, L. L. & Simoneit, B. R. T. in *Evolution of Hydrothermal Ecosystems on Earth (and Mars?): Ciba Foundation Symposium 202* 174–194 (Wiley, Chichester, 1996).
17. Summons, R. E. & Jahnke, L. L. in *Biomarkers in Sediments and Petroleum* (eds Moldowan, J. M., Albrecht, P. & Philp, R. P.) 182–200 (Prentice Hall, Englewood Cliffs, New Jersey, 1992).
18. Summons, R. E. & Walter, M. R. Molecular fossils and microfossils of prokaryotes and protists from Proterozoic sediments. *Am. J. Sci. A* **290,** 212–244 (1990).
19. Bauld, J. in *Microbial Mats: Stromatolites* (eds Cohen, Y., Castenholz, R. W. & Halverson, H. O.) 39–58 (Alan Liss, New York, 1984).
20. Kenig, F. *et al.* Occurrence and origin of mono-, di-, and trimethylalkanes in modern and Holocene cyanobacterial mats from Abu Dhabi, United Arab Emirates. *Geochim. Cosmochim. Acta* **59,** 2999–3015 (1995).
21. Golubic, S. in *Early Life on Earth: Nobel Symposium No 84* (ed. Bengtson, S.) 220–236 (Columbia Univ. Press, New York, 1994).
22. Hayes, J. M., Summons, R. E., Strauss, H., Des Marais, D. J. & Lambert, I. B. in *The Proterozoic Biosphere: A Multidisciplinary Study* (eds Schopf, J. W. & Klein, C.) 81–133 (Cambridge Univ. Press, 1992.
23. Buick, R., Rasmussen, B. & Krapez, B. Archean oil: evidence for extensive hydrocarbon generation and migration 2.5–3.5 Ga. *AAPG Bull.* **82,** 50–69 (1998).
24. Price, L. C. Thermal stability of hydrocarbons in nature: limits, evidence, characteristics, and possible controls. *Geochim. Cosmochim. Acta* **57,** 3261–3280 (1993).
25. Haug, G. H. *et al.* Glacial/interglacial variations in production and nitrogen fixation in the Cariaco Basin during the last 580 kyr. *Paleooceanography* **13,** 427–432 (1998).
26. Bisseret, P., Zundel, M. & Rohmer, M. Prokaryotic triterpenoids: 2. 2β-methylhopanoids from *Methylobacterium organophilum* and *Nostoc muscorum*, a new series of prokaryotic triterpenoids. *Eur. J. Biochem.* **150,** 29–34 (1985).
27. Zhao, N. *et al.* Structures of two bacteriohopanoids with acyclic pentol side-chains from the cyanobacterium *Nostoc* PCC 6720. *Tetrahedron* **52,** 2772–2778 (1996).
28. Llopiz, P., Jürgens, U. J. & Rohmer, M. Prokaryotic triterpenoids: Bacteriohopanetetrol glycuronosides from the thermophilic cyanobacterium *Synechococcus* PCC6907. *FEMS Microbiol. Lett.* **140,** 199–202 (1996).

Acknowledgements. We thank D. Taylor for providing Hamersley basin samples and associated geological and maturity data. M. Rohmer, J. Hayes, K. Hinrichs, A. Knoll and M. Walter provided critical and constructive comments on drafts of this manuscript.

Correspondence and requests for material should be addressed to R.E.S. (e-mail: Roger.Summons@agso.gov.au).

Spatial scaling laws yield a synthetic theory of biodiversity

Mark E. Ritchie* & Han Olff†

* *Department of Fisheries and Wildlife, Utah State University, Logan, Utah 84322-5210, USA*

† *Tropical Nature Conservation and Vertebrate Ecology Group, Department of Environmental Science, Wageningen Agricultural University, Bornsesteeg 69, 6708 PD Wageningen, The Netherlands*

Ecologists still search for common principles that predict well-known responses of biological diversity to different factors[1–4]. Such factors include the number of available niches in space[5–7], productivity[8–10], area[10], species' body size[11–14] and habitat fragmentation. Here we show that all these patterns can arise from simple constraints on how organisms acquire resources in space. We use spatial scaling laws to describe how species of different sizes find food in patches of varying size and resource concentration. We then derive a mathematical rule for the minimum similarity in size of species that share these resources. This packing rule yields a theory of species diversity that predicts relations between diversity and productivity more effectively than previous models[8–10]. Size and diversity patterns for locally coexisting East African grazing mammals and North American savanna plants strongly support these predictions. The theory also predicts relations between diversity and area and between diversity and habitat fragmentation. Thus, spatial scaling laws provide potentially unifying first principles that may explain many important patterns of species diversity.

The search for a 'unified' theory of diversity[1–5] has focused on the premise that more species can exist within a habitat whenever they can more finely divide up space and different-sized resource 'packages'. Such partitioning may be constrained by the different body sizes of species[5,7,11,12–14], but the mechanisms by which organism size, resource availability and spatial structure of habitats control species diversity remain unclear[1,2,7,11,14]. Here we employ spatial scaling laws to describe how species with different body sizes find resources in space, and how limits to the similarity in body size between any two species predicts the potential number of species in a community.

Individual organisms must search within a space of suitable physical/chemical conditions (habitat) to find resources, which are often only available inside other material (food) (Fig. 1). Therefore, resources available to organisms are nested within food, and available food is nested within habitat. For example, insect herbivores move through suitable microclimates on terres-